ATLANTIS PRESS

*Advances in Computer Science Research, volume 92*

International Conference on Mathematics, Big Data Analysis and Simulation and Modeling (MBDASM 2019)

# Research on Optimal Dispatching Simulation Model of Active Distribution Network

Yunmin Wang[1], Zaixin Yang[1], Jiangping Wang[1], Ziwen Liang[2,*] and Zihao Wang[2]

[1]Inner Mongolia Enterprise Key Laboratory of Smart Grid Simulation of Electrical Power System, Inner Mongolia Electric Power Research Institute, Hohhot, China

[2]College of Electronics and Information Engineering, Tongji University, Shanghai, China

[*]Corresponding author

***Abstract*—It is a technical difficulty for the safe and economic running of active distribution network to control and manage distributed generators, energy storage system and load flexibly and effectively to eliminate the effect of distributed energy uncertainty on grid. In order to achieve the optimal coordinated control of active distribution network, a topology structure of active distribution network based on improved IEEE 33 nodes network is established. Including photovoltaic power generation systems, wind power generation system and energy storage system, a simulation model of active distribution network is built by using PSCAD/EMTDC. By adopting the optimized control strategy of the converter, the voltage of each node in active distribution network is stable, thus the validity and stability of the model are verified.**

***Keywords—active distribution network; dispatching control; photovoltaic generation system; wind turbine system; energy storage system***

## I. INTRODUCTION

In recent years, with the depletion of fossil energy sources and the serious environmental pollution caused by the use of these fossil energy sources, renewable energy sources such as wind, solar and geothermal energy have developed rapidly [1, 2]. Distributed energy resources (DER) is the collective name of distributed generation (DG), electrical energy storage (EES) and controllable load (CL), among which DG is mainly renewable energy, including solar power, wind power, etc. [3]. With the large number of DGs merged into distribution network, the traditional distribution network with unidirectional power flow is gradually transformed into the active distribution network (ADN) with DG and bidirectional power flow, which is the main development trend and mode of distribution network in the future [4, 5].

ADN has the characteristics of flexible topology, controllable power flow, flexible access and consumption of a large number of DGs. Meanwhile, it can improve the optimal allocation ability of energy transmission network, and the quality and reliability of power supplied for users. Because ADN contains a great qantity of DGs, it is necessary to study the optimal dispatching model of ADN and the management and control of demand side response. The premise is to establish a correct distributed power source model and analyze their characteristics. Ref. [6] models the internal source, load and storage of ADN as agents, and constructs the coordinated optimal operation model of active distribution network source-load-storage, but focuses on the analysis and comparison of distributed control methods of active distribution network. In [7], an improved multi-parameter planning method is proposed for the coordinated dispatch problem of transmission and distribution, but the uncertainty of large-scale distributed generation centralized access to transmission network is not considered. Ref. [8] simplifies the wind turbine model and only considers aerodynamic characteristics. The mathematical expression of mechanical power of wind turbine with wind energy utilization coefficient is obtained, but the randomness and fluctuation of wind power generation are not considered.

In order to realize optimal dispatching control of active distribution network, this paper establishes mathematical models of photovoltaic cells, wind turbines and batteries. And an active distribution network topology based on improved IEEE 33 node network is established. Then a simulation model of active distribution network including photovoltaic power generation system, wind power generation system, energy storage system, lines and loads is built. In the simulation model, the optimized control strategy of grid-connected converter is introduced to effectively stabilize the voltage fluctuation of distribution network. The voltage fluctuation and harmonic of the grid-connected points of distributed generation and the typical nodes of the system are simulated, and the validity of the model is verified.

## II. THE TOPOLOGY OF ACTIVE DISTRIBUTION NETWORK

Besides the generators, lines, transformers, capacitors and other electrical components in the traditional power grid, active distribution network also contains a variety of DGs. However, many DGs are characterized by intermittent, fluctuating and unpredictable power output. Photovoltaic(PV) generation systems and wind turbine(WT) generation systems are generally considered as the typical representative of DGs. So in the actual operation of active distribution network, it is necessary to configure EES to suppress distributed generation fluctuations and reduce the load spikes in the high penetration or heavy load areas of distributed power generation.

So far there is no unified active distribution network model, and the model is based on demonstration distribution networks or IEEE standard distribution systems in general. Among them, the IEEE 33 bus system is typical and widely used. Based on the characteristics of active distribution network, distributed energy allocation and expansion are carried out on the basis of IEEE 33 node system. The original load in IEEE 33 is taken as the basic load of distribution network, and renewable distributed generation and energy storage unit are connected to simulate the basic composition of ADN. An ADN topology is constructed, as shown in Figure 1.

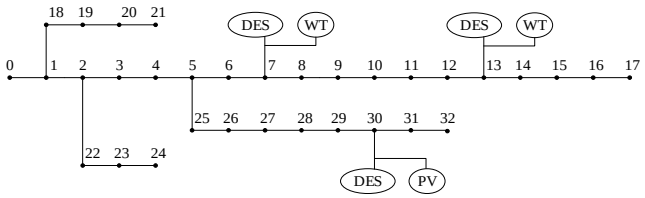


FIGURE I. AN IEEE 33 NODES DISTRIBUTION NETWORK EXAMPLE SYSTEM

In Figure 1, the load parameters of each node are consistent with those of the original IEEE 33 node. A set of wind power generation systems and energy storage systems are added to node 7 and node 13, and a set of photovoltaic power generation systems and energy storage systems are added to node 30. The specific parameters of each distributed generators are shown in Table I. Loads 7, Loads 8, Loads 30 and Loads 32 are commercial loads, loads 24 and Loads 25 are industrial loads, and the remaining nodes are residential loads.

TABLE I. DISTRIBUTED POWER CONFIGURATION PARAMETERS

| Node | Type of Power | Capacity |
|---|---|---|
| 7 | Wind power generation | 500kW |
| 7 | Battery energy storage | 500 kWh |
| 13 | Wind power generation | 500 kW |
| 13 | Battery energy storage | 500 kWh |
| 30 | Photovoltaic power generation | 500 kW |
| 30 | Battery energy storage | 500 kWh |

## III. THE MODEL OF DISTRIBUTED ENERGY

### *A. The Model of Photovoltaic Power Generation System*

Photovoltaic power generation systems are generally composed of photovoltaic arrays, filters, inverters, etc. Photovoltaic cells convert solar energy into electrical energy through uncontrolled rectification, boost converter, application of Maximum Power Point Tracking (MPPT) method. Finally the photovoltaic power generation system is connected to the grid through the inverter, as shown in Figure 2.

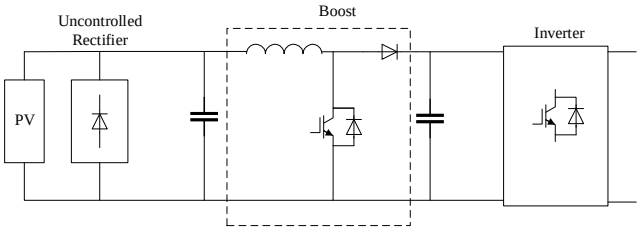


FIGURE II. THE STRUCTURE OF PHOTOVOLTAIC POWER GENERATION SYSTEM

*1) The mathematical model of photovoltaic cells*

The photovoltaic cell is the core part of solar power generation system. The output of a photovoltaic cell relies on its rated power $G_{rate}$, illumination $S$ and environmental temperature $E$:

$$G_S = \frac{S}{S_{rate}} \cdot \eta(E) \cdot G_{rate} \tag{1}$$

$$\eta(E) = \left[1 - 0.0045 \cdot (E - E_{rate})\right] \tag{2}$$

where $S_{rate}$ is the rated value of solar radiation, efficiency factor $\eta(E)$ is defined to quantify the impacts of $E$, and reference temperature $E_{rate}$ is commonly set to 25 ℃.

The equivalent circuit is used to indicate the relevant characteristics of the photovoltaic cells, of which the single diode equivalent circuit is used mostly, as shown in Figure 3.

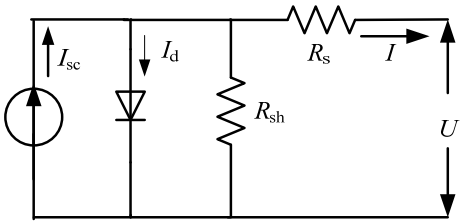


FIGURE III. THE EQUIVALENT CIRCUIT OF PHOTOVOLTAIC CELLS

According to Fig. 3, the output current expression of the photovoltaic cells can be obtained:

$$I = I_{sc} - I_d\left(\exp\left(\frac{q(U + IR_s)}{AKT}\right) - 1\right) - \frac{U + IR_s}{R_{sh}} \tag{3}$$

Where $I$ is the current flowing through the load, $I_{sc}$ is a photo-generated current proportional to the intensity of sunshine, $I_d$ is reverse saturation current (order of magnitude $10^{-4}$ A), $q$ is the electronic load ($1.6\times10^{-19}$C), $K$ is the Boltzmann constant ($1.38\times10^{-23}$J/k), $T$ is the absolute temperature, $A$ is the P-N junction ideal factor, $R_{sh}$ is the parallel resistance of the photovoltaic cell, $R_s$ is the series resistance of the photovoltaic cell.

*2) Maximum Power Point Tracking (MPPT)*

The maximum power point tracking of photovoltaic power generation technology is aimed at achieving the maximum output power in different cases. In this paper, the conductance increment method is used to achieve MPPT. The implementation process is shown in Figure 4.

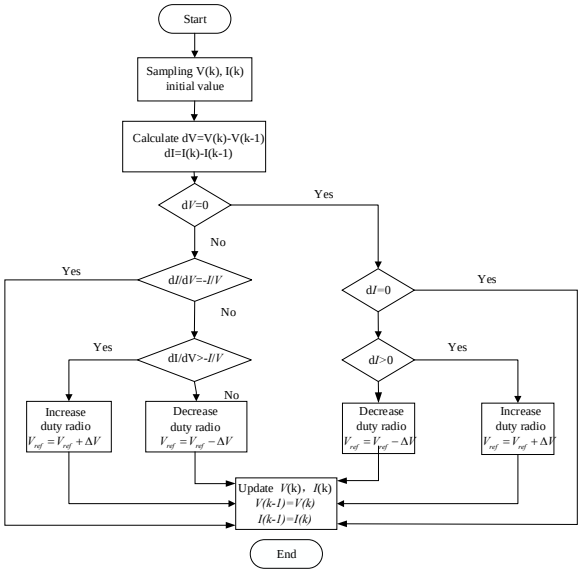


FIGURE IV. THE FLOW CHART OF CONDUCTION INCREMENT METHOD

*B. The Model of Wind Turbine System*

Permanent magnet synchronous generators (PMSG) are widely used in small- and medium-sized wind turbines because of its simple structure, no excitation winding and high efficiency. With the improvement of high performance magnet material manufacturing technology, large capacity wind power system tends to use PMSG. Therefore, PMSG is selected in this paper, which is composed of wind turbine, direct drive PMSG, full power converter and other devices, as shown in Figure 5. The wind turbine drives the synchronous generator to run, and the electric energy caused by the synchronous generator is converted into power-frequency through AC-DC-AC converter, and then connected to the grid after passing through the filter device and isolation transformer.

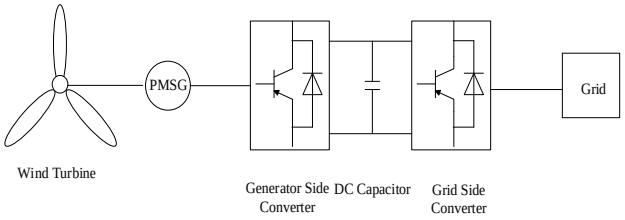


FIGURE V. THE STRUCTURE OF WIND POWER SYSTEM

*1) The model of wind turbine*

Wind turbines convert the wind energy into mechanical energy, which is then converted into electrical energy by permanent magnet synchronous motors.

The output mechanical power of wind turbine $P_m$:

$$P_m = 0.5 C_p \rho \pi R^2 v^3 \tag{4}$$

The ratio of blade tip linear velocity to wind speed is called tip velocity ratio:

$$\lambda = \frac{wR}{v} \tag{5}$$

The output power of wind turbine $P$:

$$P = \eta P_m \tag{6}$$

where $C_p$ is the utilization coefficient of wind energy, $\eta$ is the efficiency of WT, $\rho$ is air density(kg/m$^2$), $R$ is radius of the wind turbine (m), $v$ is wind speed (m/s).

Considering that the power regulation of wind turbines completely depends on the aerodynamic characteristics of blades and speed regulating devices, wind energy captured by wind turbines and speed of wind turbines are limited. Further considering the fluctuation of wind speed and direction in the wind field, the theoretical output power of the wind turbine can be obtained:

$$P = \begin{cases} 0.5 C_p \rho V A^3, & V_{in} < V < V_e \\ P_e, & V_{in} < V < V_{out} \\ 0, & V \geq V_{out} \end{cases} \tag{7}$$

where $V_{in}$, $V_e$ and $V_{out}$ are wind turbine cut-in wind speed, rated wind speed and cut-out wind speed, $P_e$ is rated power of wind turbine, $A=\pi R^2$ is the area swept by the blade.

*2) The model of generator*

The stator voltage equation of permanent magnet synchronous motor in d/q rotating coordinate system can be expressed as follows:

$$\begin{cases} U_{sd} = -R_s i_d + \omega_r L_q i_q - L_d \dfrac{di_d}{dt} \\ U_{sq} = -R_s i_q - \omega_r L_d i_d - L_q \dfrac{di_q}{dt} + \omega_r \varphi_f \end{cases} \tag{8}$$

The mathematical model of permanent magnet synchronous motor in d/q rotating coordinate system is as follows:

$$\begin{cases} \dfrac{di_d}{dt} = \dfrac{1}{L_{md}+L_{is}}\left[-R_s i_d + \omega_r (L_{mq}+L_{is}) i_q + U_d\right] \\ \dfrac{di_q}{dt} = \dfrac{1}{L_{mq}+L_{is}}\left[-R_s i_q + \omega_r (L_{md}+L_{is}) i_d + U_q - \omega_r \varphi_f\right] \end{cases} \quad (9)$$

The electromagnetic torque produced by the PMSG is as follows:

$$T_e = 1.5p\left[\left(L_{md}-L_{mq}\right) i_d i_q + \varphi_f i_q\right] \quad (10)$$

where $U_d$ is the d axis generator terminal voltage component, $U_q$ is the q axis generator terminal voltage component, $\omega_r$ is angular velocity of rotation of rotor, $R_s$ is stator resistance, $L_{md}$ and $L_{mq}$ are the d axis and q axis inductance of stator, $L_{is}$ is the stator leakage reactance, $\phi_f$ is the permanent magnetic flux, $p$ is the number of pole-pairs.

### C. The Model of Battery Energy Storage System

The most widely applicable model of battery energy storage system is the internal resistance model. The equivalent circuit of the model is shown in Figure 6.

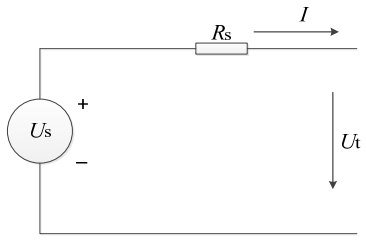


FIGURE VI. THE EQUIVALENT CIRCUIT OF INTERNAL RESISTANCE MODEL

In Figure 6, $U_s$ is the ideal voltage source, $R_s$ is the internal resistance of battery, $U_t$ is the terminal voltage of battery, $I$ is the charging and discharging current.

The following equation can be obtained from Figure 6:

$$U_t = U_s - IR_s \quad (11)$$

Supposing that $U_s$ and $R_s$ are the linear functions of SOC (State of Charge), which can be expressed by the following equations:

$$U_s = U_{oc} - K_u\left(1-SOC\right) \quad (12)$$

$$R_s = R_0 - K_r\left(1-SOC\right) \quad (13)$$

where $U_{oc}$ is the open-circuit voltage when the battery is fully charged (SOC = l), $R_0$ is the internal resistance, $K_u$ and $K_r$ can be determined by constant current discharge test.

By substituting (12) and (13) into (11), $U_t$ can be expressed as showing in (14):

$$U_t = U_{oc} - IR_0 - \left(K_u - K_r\right)\left(1-SOC\right) \quad (14)$$

### D. Optimized Control Strategy of Inverter

Since the photovoltaic cells and batteries output direct current, an inverter composed of power electronic devices is required to convert DC to AC, then integrated into the active distribution network. The boost circuit is shown in Figure 7, and the relationship between duty cycle and output voltage is as follows:

$$G_{vd}(s) = \frac{v(s)}{d(s)} = \frac{U_g}{D'^2}\frac{(1-\frac{sL}{D'^2R})(1+sR_cC)}{1+s/Q\omega_0+s^2/\omega_0^2} \quad (15)$$

$$Q = \frac{1}{\omega_0[\frac{L}{D'^2R}+(R_c+\frac{R_L}{D'^2})C]} \quad (16)$$

$$\omega_0 = \frac{1\text{-}D}{\sqrt{LC}} \quad (17)$$

where $M$ is the transformer ratio, $U_g$ is the input voltage, $D$ is the duty cycle.

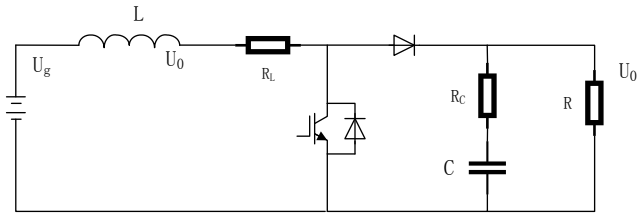


FIGURE VII. THE BOOST CIRCUIT

When a fault occurs in the system, PQ-IIDG should output a certain reactive power to support the stable operation of the system by considering LVRT(low voltage ride through) and system parameters of the ADN [9]. For the sake of improve the output characteristics of PQ-IIDG, an optimized control strategy based on the positive-sequence component is adopted, and the output reactive and active currents of PQ-IIDG can be expressed as follows:

$$I_{\mathrm{q}}=\begin{cases}0, & 0.9U_e<U_{d,f}^{+}\le U_e\\ 2I_{\max}(1-\dfrac{U_{d,f}^{+}}{U_e}), & 0.5U_e<U_{d,f}^{+}\le 0.9U_e\\ I_{\max}, & 0\le U_{d,f}^{+}\le 0.5U_e\end{cases} \quad (18)$$

$$I_{\mathrm{d}}=\begin{cases}\mathrm{P}_{ref}/U_{d,f}^{+}, & 0.9U_e<U_{d,f}^{+}\le U_e\\ \min(\dfrac{\mathrm{P}_{ref}}{U_{d,f}^{+}},\sqrt{I_{\max}{}^2-I_{\mathrm{q}}{}^2}), & 0.5U_e<U_{d,f}^{+}\le 0.9U_e\\ 0, & 0\le U_{d,f}^{+}\le 0.5U_e\end{cases} \quad (19)$$

where $P_{\mathrm{ref}}$ is the active power reference of PQ-IIDG, $U_e$ is the rated voltage of PQ-IIDG, $U_{d,f}^{+}$ is the positive-sequence component of the grid-connected voltage after a fault occurs.

In normal operation, PQ-IIDG only outputs active current to improve the energy efficiency. According to (15)-(19), a simplified expression of $D$ and $U_{d,f}^{+}$ can be obtained:

$$D=f(U_{d,f}^{+}) \quad (20)$$

When integrated into the active distribution network, a PLL (Phase-locked loop) is required to maintain the frequency of the output as the power frequency. Meanwhile, PQ control is adopted in order to make the output power stable and controllable, and the block diagram is shown in Figure 8.

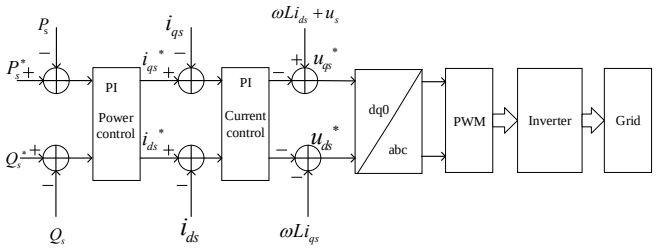


FIGURE VIII. THE PQ CONTROL STRATEGY STRUCTURE BLOCK DIAGRAM

## IV. MODELING AND SIMULATION OF ACTIVE DISTRIBUTION NETWORK

In view of the above model and optimized control strategy, the simulation model of coordinated optimization of ADN shown in Figure 1 is established in PSCAD/ EMTDC. As shown in Figure 9, the system reference voltage is 10 kV and the reference power is 10 MW.

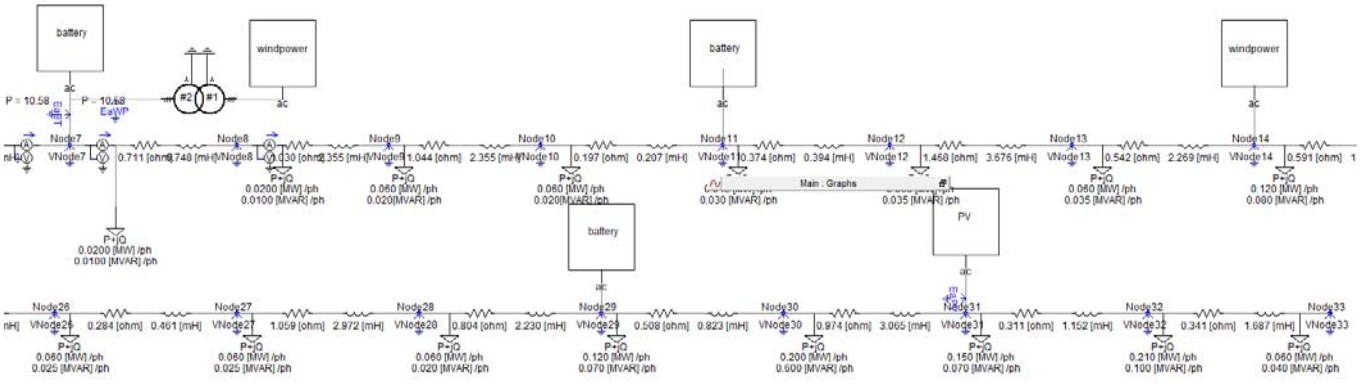


FIGURE IX. THE SIMULATION MODEL OF COORDINATED OPTIMIZATION OF ADN

### *A. The Simulation Results of Inverter Control for Photovoltaic Power Generation System*

It can be seen that photovoltaic cells convert solar energy into electrical energy, and get the expected DC side voltage through MPPT by using the above control strategy. Boost circuit increases and stabilizes the DC side voltage, providing a stable DC voltage for grid fault and abnormal situations. When the three-phase unbalanced voltage comes out in the system, the output power of photovoltaic system is shown in Figure 10. As shown in Figure 10, the active and reactive powers of photovoltaic power generation system can maintain stability, and the optimized control strategy is effective.

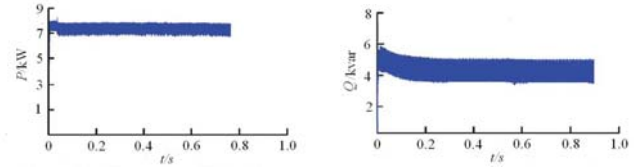


(a) active power (b) reactive power

FIGURE X. THE OUTPUT POWERS OF PHOTOVOLTAIC SYSTEM

### *B. The Simulation Results of Photovoltaic Arrays with Constant Illumination Intensity and Varying Wind Speed*

The temperature of photovoltaic cells is 50℃, the solar radiation is 1000W/m$^2$, the initial wind speed is 18m/s, the

gust is maintained for 2s and the amplitude is 9m/s. The voltage fluctuations of grid-connected points and typical nodes with DGs are simulated and analyzed as shown in Table II, and the total harmonics distortion is shown in Table III. Nodes 2, 8 and 25 are selected as typical nodes. Node 25 is located on the feeder of photovoltaic power generation system, while Node 8 is located on the right of grid-connected point of wind power generation system.

TABLE II. THE RESULTS OF VOLTAGE FLUCTUATION

| **Node** | 7 | 30 | 2 | 8 | 25 |
|---|---|---|---|---|---|
| **Before (*U*/pu)** | 1.0369 | 1.0306 | 1.0428 | 1.0311 | 1.0345 |
| **After (*U*/pu)** | 1.0446 | 1.0346 | 1.0434 | 1.0337 | 1.0389 |

TABLE III. THE RESULTS OF VOLTAGE TOTAL HARMONICS DISTORTION

| **Node** | 7 | 30 | 2 | 8 | 25 |
|---|---|---|---|---|---|
| **Before (THDv/%)** | 1.4989 | 1.4761 | 1.4635 | 1.4702 | 1.4578 |
| **After (THDv/%)** | 1.2003 | 1.0834 | 0.9796 | 1.0754 | 0.9710 |

The active power of the generator is stable at 2.26MW from 1.36s. After 2s, because of decreasing wind speed, the active power falls and stabilizes at 0.26MW. From Table II and Table III, when the wind power output decreases, the voltage amplitudes of the grid-connected points and typical nodes with DGs remain stable after the wind speed changes. Voltage fluctuation is less than ± 5% rated voltage, and the voltage total harmonic distortion is less than 4%, which satisfies the requirements of grid-connection specifications.

### *C. The Simulation Results of constant wind speed and varying solar illumination intensity*

The wind speed is 9m/s and the temperature of photovoltaic cells is 50℃. The input of solar illumination intensity changed from 600W/m$^2$ to 1000W/m$^2$ at 2s. The voltage fluctuations of grid-connected points and typical nodes with DGs are simulated and analyzed as shown in Table IV, and the total harmonic distortion of voltage is shown in Table V.

TABLE IV. THE RESULTS OF VOLTAGE FLUCTUATION

| **Node** | 7 | 30 | 2 | 8 | 25 |
|---|---|---|---|---|---|
| **Before (U/pu)** | 1.0368 | 1.0312 | 1.0421 | 1.0334 | 1.0375 |
| **After (U/pu)** | 1.0366 | 1.0329 | 1.0450 | 1.0356 | 1.0390 |

TABLE V. THE RESULTS OF VOLTAGE HARMONICS DISTORTION

| **Node** | 7 | 30 | 2 | 8 | 25 |
|---|---|---|---|---|---|
| **Before (THDv/%)** | 1.4686 | 1.4713 | 1.4435 | 1.4628 | 1.4465 |
| **After (THDv/%)** | 2.5651 | 2.6127 | 2.4662 | 2.5204 | 2.4859 |

At 1.63s, the output active power of PV cells is basically stable at 0.25MW. After 2s, the active power increased to 0.48MW due to the increase of solar radiation. Table IV and Table V shows that the voltages of each grid-connected point and each typical node does not fluctuate significantly when the photovoltaic output increases which can maintain a relatively stable state. Voltage fluctuation is less than ± 5% rated voltage. With the increase of output power, the total harmonic distortion of voltage increases but less than 4%, which meets the requirements of grid-connected specifications.

## V. CONCLUSION

According to the main characteristics of ADN, this paper establishes an ADN topology based on IEEE 33 bus system, builds an ADN simulation model including PV system, WT generation system and energy storage system. An optimized grid-connected converter control strategy is presented. The simulation results show that the model satisfies the requirements of IEEEStd.1547-2003 grid-connected specifications and power quality which verifies the validity and correctness of the model. The study provides support for the optimal dispatching control of ADN.

## ACKNOWLEDGMENT

Project supported by the Science & Technology Program of Inner Mongolia Power (Group) Co., Ltd(Science & Technology Information Department of Inner Mongolia Power Company:〔2018〕47).

## REFERENCES

[1] BAI Jianhua, XIN Songxu, LIU Jun, ZHENG kuan. Roadmap of realizing the high penetration renewable energy in China. Proceedings of the CSEE, 2015, 35(14): 3699-3705.

[2] S. Chu, A. Majumdar. Opportunities and challenges for a sustainable energy future. Nature, 2012, 488(7411): 294-303.

[3] FAN Mingtian, ZHANG Zuping, SU Aoxue, SU Jian. Enabling technologies for active distribution systems. Proceedings of the CSEE, 2013, 36(22): 12-18.

[4] ZHAO Junhui, WANG Caisheng, ZHAO Bo, Feng Lin, Quan Zhou, Yang Wang. A review of active management for distribution networks: current status and future development trends. Electric Power Components and Systems, 2014, 42(3-4): 280-293.

[5] You Yi, LIU Dong, YU Wenpeng, Chen Fei, PAN Fei. Technology and its trends of active distribution network. Automation of Electric Power Systems, 2012, 36(18): 10-16.

[6] Xu Xilin, Song Yiqun, Yao Liangzhong, YAN Zheng. Source-load-storage distributed coordinative optimization of AND(part I): consensus based distributed coordination system modeling. Proceedings of the CSEE, 2018, 38(10): 2841-2848+3135.

[7] LIN Chenhui, WU Wenchuan, CHEN Xin, ZHENG Weiye. Decentralized dynamic economic dispatch for integrated transmission and active distribution networks using multi-parametric programming. IEEE Transactions on Smart Grid, 2018, 9(5): 4983-4993.

[8] CHEN Pengwei, TAO Shun, XIAO Xiangning, WANG Zhiqiang. Source-load model improvement and parallel computing for reliability evaluation of active distributed networks. Automation of Electric Power Systems, 2016, 40(18): 68-75.

[9] Calderaro V, Conio G, Galdi V, Massa G, Piccolo A. Active management of renewable energy sources for maximizing power production. International Journal of Electrical Power & Energy Systems, 2014, 57: 64-72.